© 2017. Published by The Company of Biologists Ltd | Journal of Experimental Biology (2017) 220, 2787-2797 doi:10.1242/jeb.153783

RESEARCH ARTICLE

Labrid cleaner fishes show kinematic convergence as juveniles despite variation in morphology

Vikram B. Baliga[1,*], Ze'ev J. Bernstein[2], Shivani Sundaram[3] and Rita S. Mehta[1]

ABSTRACT

Cleaning, a dietary strategy in which mucus or ectoparasites are removed and consumed off other taxa, is performed facultatively or obligately in a variety of species. We explored whether species in the Labridae (wrasses, parrotfishes) of varying ecological specialization employ similar mechanisms of prey capture. In investigating feeding on attached prey among juveniles of 19 species of wrasses, we found that patterns of biting in wrasses are influenced by the interaction between the maxilla and a feature of the premaxilla which we term the maxillary crest. Premaxillary motion during biting appears to be guided by the relative size of the crest. In many cases, this results in a 'premaxillary bite' wherein the premaxillae rapidly move anteroventrally to meet the lower jaws and deliver a protruded bite. Cleaners in the Labrichthyini tribe, however, exhibited reduced or absent maxillary crests. This coincided with a distinct kinematic pattern of prey capture in these labrichthyine cleaners, coupled with some of the fastest and lowest-excursion jaw movements. Although evidence of kinematic specialization can be found in these labrichthyines (most notably in the obligate cleaners in *Labroides*), we found that facultative cleaners from other lineages similarly evolved reductions in excursions and timing. Convergence in feeding kinematics is thus apparent despite varying degrees of cleaning specialization and underlying morphological features.

KEY WORDS: Cleaning, Feeding kinematics, Protruded biting, Convergent evolution, Jaw protrusion, Wrasses

INTRODUCTION

The ecological specialization of species is an important driver of phenotypic evolution (Haldane, 1951; Futuyma and Moreno, 1988; Martin and Wainwright, 2011; Armbruster, 2014). Adaptive radiation, among other processes, can lead to increases in phenotypic diversity as taxa begin to specialize within distinct niches. In contrast, the repeated evolution of a particular specialization could result in convergent evolution among taxa, reducing phenotypic variance. Such reductions may be especially pronounced in cases where the ability to occupy a certain niche is coupled strongly with functional constraints.

Naturally, the extent of ecological specialization can vary widely among species. True 'specialists' (i.e. those that show highly specific ecological roles) might be expected to exhibit morphological, behavioral and/or physiological adaptations to aid in the task at hand. Alternatively, species that engage in an ecological role facultatively may not necessarily experience sustained selection for the same suite of functional traits shown by specialists.

The evolution of cleaning behavior in labrids offers a chance to understand how the extent of specialization can influence patterns of functional convergence. Do species of varying specialization employ similar mechanisms of prey capture? In fishes, cleaning is a dietary strategy that involves the removal and consumption of ectoparasites (and, in many instances, mucus and scales) off other organisms. Although over 120 species of marine teleost fishes clean, the majority (87.7%) exhibit this behavior facultatively (Coté, 2000).

The Labridae (wrasses, parrotfishes and odacids) in particular provide an exemplary system in which to explore how varying levels of specialization may relate to functional convergence. At least 59 species of labrids exhibit cleaning behavior (Coté, 2000; Baliga and Law, 2016). Phylogenetic inference reveals that the feeding strategy has evolved at least 26 times in this group (Baliga and Law, 2016). Across this diversity, the extent to which cleaning occurs varies. The predominant pattern (74.2% of cleaner species) is juvenile cleaning, wherein species clean facultatively as juveniles and exhibit shifts away from this strategy as adults. Facultative cleaning throughout ontogeny is less common (19.0%). Obligate cleaning (8.6%), wherein nearly all dietary items are obtained through cleaning interactions, is exclusively observed (throughout ontogeny) in the five species of *Labroides* that are found within the Labrichthyini tribe of wrasses (Russell, 1988; Westneat and Alfaro, 2005). As labrids that clean are all expected to do so as juveniles (and some may continue as adults), studying functional convergence warrants comparisons across juvenile individuals of taxa.

Previous observations of feeding kinematics in cleaners helped guide our present approach. Baliga and Mehta (2015) found that in three labrids that clean, prey capture relied on the ability to perform fast, low-displacement biting. This allowed for rapid and multiple gape cycles on individually targeted items. Preliminary evidence suggested that there may be additional morphological and behavioral adaptations that could enhance ectoparasitivory. For example, *Labroides dimidiatus* and *Larabicus quadrilineatus* (both labrichthyine wrasses) exhibited relatively acute angles of approach to bite prey through an opening made by a vertical midline cleft in the lower lips. These features were absent in a non-labrichthyine cleaner, *Thalassoma lutescens*. Conceivably, labrichthyine wrasses (the only clade to include highly specialized obligate cleaners) possess morphological and biomechanical feeding adaptations not observed in other labrid cleaners.

The prevalence and diversity of cleaning in the Labridae afforded us the opportunity to expand on previous findings and assess broader morphological and kinematic patterns of cleaners (Baliga and Mehta, 2015). We also observed feeding events from closely related non-cleaner taxa to help contextualize behaviors. Using a phylogenetic comparative framework, we tested hypotheses of

[1]Department of Ecology and Evolutionary Biology, Long Marine Laboratory, University of California Santa Cruz, 100 Shaffer Road, Santa Cruz, CA 95060, USA. [2]Pacific Collegiate School, 3004 Mission Street, Santa Cruz, CA 95060, USA. [3]Monta Vista High School, 21840 McClellan Rd, Cupertino, CA 95014, USA.

*Author for correspondence (vbaliga@ucsc.edu)

V.B.B., 0000-0002-9367-8974

Received 24 November 2016; Accepted 14 May 2017

Journal of Experimental Biology (2017) 220, 2787-2797 doi:10.1242/jeb.153783

mean differences between cleaners and non-cleaners in all measured kinematic variables. We also tested the association between body orientation angle and the presence of a cleft in the lower lips. Our selection of taxa and feeding protocol also led us to identify distinct patterns of biting behaviors and then provide hypotheses on their fundamental mechanisms. As detailed herein, we observed two general patterns of upper jaw movement during biting. In one pattern ('premaxillary biting', shared by many diverse genera), the upper jaws, while protruded, moved rapidly in an anteroventral direction to bite down on prey. In the other pattern, shown only by labrichthyine wrasses, biting occurred as the upper jaws had returned to a nearly non-protruded state. Through dissections and manipulations of prepared specimens, we hypothesized that a feature of the premaxilla, which we term the 'maxillary crest of the premaxilla' (MXC), guides the motion of the upper jaws. We therefore tested hypotheses that the size of the MXC was correlated with three kinematic variables: time to peak premaxillary protrusion, peak premaxillary protrusion and time to jaw retraction. Lastly, we aimed to determine the extent to which labrid cleaners exhibit kinematic convergence despite the apparent dichotomy of upper jaw movement patterns between the labrichthyines and other wrasses.

MATERIALS AND METHODS

We collected data from 19 species of labrids, 10 of which are known to exhibit cleaning behavior (Fig. 1A; Table S1) (Baliga and Law, 2016). Because most of these cleaners clean predominantly as juveniles (Coté, 2000; Baliga and Law, 2016), we obtained juvenile individuals for all species. Our sampling included four members (*Diproctacanthus xanthurus*, *L. quadrilineatus*, *Labroides pectoralis* and *L. dimidiatus*) of the tribe Labrichthyini (Russell, 1988; Westneat and Alfaro, 2005), a clade notable for containing the only obligate cleaner wrasses. We obtained all fishes (5 individuals per species; 95 total individuals) through the aquarium trade. Fishes were housed and filmed at the Long Marine Laboratory, University of California, Santa Cruz, following IACUC protocol (IACUC no. 1009).

Phylogenetic relationships between 320 wrasses, including the 19 taxa in the present study, were previously inferred by Baliga and Law (2016) and informed our analyses. Inference of the evolutionary history of cleaning (via stochastic character mapping) was originally performed by Baliga and Law (2016). Trees and character histories were then pruned to the 19 focal taxa in our study. Additional character histories were performed for other traits (see below).

Collection of kinematic data

All individuals were trained to feed on a mixture of thawed bloodworms and mysis shrimp embedded manually into a wire mesh. We recorded feeding behaviors after individuals had been trained to feed in this manner, generally between 1 and 4 days. We filmed lateral profiles of feeding using a Photron FASTCAM SA3 high-speed video camera (Photron, Tokyo, Japan) at 1000 frames s^{-1} at 1024×1024 pixel resolution. Two 5000 lm lights were used to illuminate the feeding apparatus. To calibrate measurements, we recorded a still image of a ruler in the water column without adjusting the focus, zoom or height of the camera.

We used Tracker (http://physlets.org/tracker/) to digitize a total of 950 feeding sequences (10 sequences per individual fish). We acquired data from trials in which a successful strike occurred, a lateral view of the fish was available over the entire sequence and all landmarks were visible. A trial was considered successful if an individual removed a piece of prey from the wire mesh. We defined time zero as the frame before initial jaw opening and defined the end of the strike as the frame in which the jaws returned into their original positions and orientations.

Seven external landmarks were used to quantify principal kinematic variables (Fig. 2). The landmarks were: (1) the anterior tip of the premaxilla, (2) the posterior margin of the nasal bone, (3) the (approximate) point of articulation between the hyomandibula and the neurocranium, (4) the anterior insertion of the pelvic fin, (5) the (approximate) articulation of the lower jaw with the quadrate, (6) the anteroventral protrusion of the hyoid and (7) the anterior tip of the dentary. We employed the automated tracking feature within

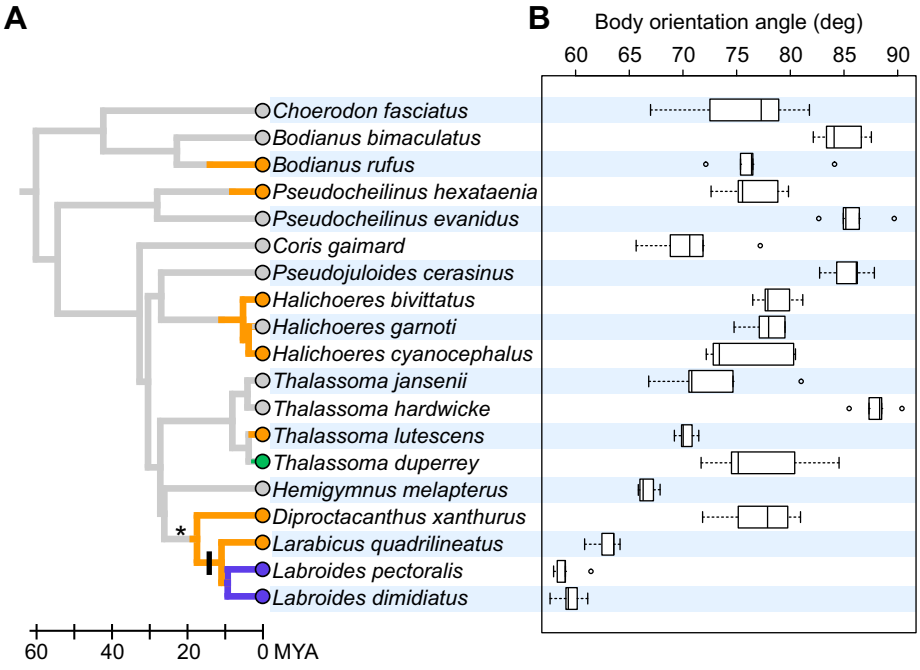

Fig. 1. Phylogenetic relationships between taxa and body orientation angles shown during feeding. (A) Phylogenetic relationships between 320 wrasses, including the 19 taxa in our study, were previously determined by Baliga and Law (2016). Inference of the evolutionary history of cleaning, accomplished via stochastic character mapping, was originally performed by Baliga and Law (2016). Phylogenetic trees and character histories were then pruned to the 19 focal taxa in our study. The asterisk indicates the common ancestor of labrichthyine taxa in this study. A single stochastic character map is painted along the branches of the tree. Colors correspond to distinct characters: obligate cleaning is purple; facultative cleaning (throughout ontogeny) is green; juvenile cleaning is orange; and non-cleaning is gray. Inference of the evolution of a complete cleft bisecting the lower lip is shown with a vertical black bar. (B) Distribution of body orientation angles of predators, depicted using boxplots. Mean data from all individuals are shown and pooled together at the species level.

Journal of Experimental Biology

Journal of Experimental Biology (2017) 220, 2787-2797 doi:10.1242/jeb.153783

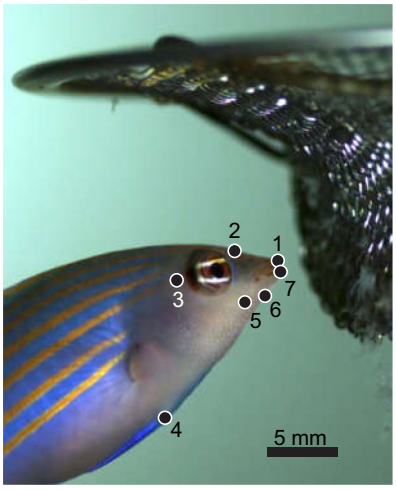

Fig. 2. Landmarks used during kinematic analyses. Still image of *Pseudocheilinus hexataenia* features the following landmarks: (1) the anterior tip of the premaxilla, (2) the posterior margin of the nasal bone, (3) the (approximate) point of articulation between of the hyomandibula and the neurocranium, (4) the dorsal margin of the insertion of the pelvic fin (a reference point), (5) the (approximate) articulation of the lower jaw with the quadrate (i.e. the jaw joint), (6) the anteroventral protrusion of the hyoid and (7) the anterior tip of the dentary (lower jaw).

Tracker to monitor changes in the positions of the seven landmarks for the quantification of three excursion variables, three angular variables and their associated timing. Landmarks were digitized for each frame for the collection of data every 1 ms. After the automated tracking concluded, we manually examined each point to ensure accuracy.

The excursion variables (in mm) were: gape distance, premaxillary protrusion distance and hyoid excursion distance. Gape distance was defined as the change in distance between the upper and lower jaw tips (landmarks 1 and 7). Premaxillary protrusion distance was the change in distance between the upper jaw tip and the posterior margin of the nasal bone (landmarks 1 and 2). Following Ferry-Graham et al. (2002), hyoid excursion distance was measured as the net change in straight-line distance between the anteroventral protrusion of the hyoid and the approximate point of articulation between the hyomandibula and the neurocranium (landmarks 3 and 6).

The angular displacement variables (in deg) were: lower jaw rotation (landmarks 2, 5, 7) and cranial rotation (landmarks 2, 3, 4). The variables were measured following Baliga and Mehta (2015) and taken as the net change in an angle relative to its pre-jaw opening value. In addition, we measured the body orientation angle (the angle between the midline of the fish's cranium and the surface of the suspended wire mesh) at the onset of jaw opening, following Baliga and Mehta (2015).

The timing variables (in ms) were: time to peak gape, time to peak premaxillary protrusion, time to peak lower jaw rotation, time to peak cranial rotation, time to peak hyoid excursion and time to jaw retraction (end of strike).

Collection of morphological data

After filming, we killed each fish via an overdose of MS-222 (IACUC no. 1006). We assessed whether specimens possessed midline clefts in the lower lips following Baliga and Mehta (2015). We then placed freshly killed specimens under a light microscope and manually manipulated their jaws to observe potential mechanisms of jaw protrusion and jaw closing. Anatomical descriptions of cranial features, including the nomenclature of muscles, bones and ligaments, follow Winterbottom (1974), Tedman (1980a,b), Westneat (1990, 1994) and Baliga and Mehta (2015). Each specimen was then fixed in 10% buffered formalin and subsequently cleared and double-stained for bone and cartilage following a modification of Dingerkus and Uhler (1977). We performed additional manipulations of the jaws on cleared and stained specimens to further understand jaw movements.

We hypothesized that the relative size of a feature we named the MXC was an important determinant of how the premaxilla interacts with the maxilla during upper jaw motion, affecting timing and excursion of the jaws (see Results and Discussion for further details). This crest is found along the dorsolateral edge of the ascending process of the premaxilla in most taxa studied herein. To capture the size of the MXC, we first parameterized premaxillary shape using geometric morphometrics. Four landmarks were placed on lateral photographs of each specimen (Fig. S1): the distal end of the ascending process, the intersection of the ascending and alveolar processes, the distal end of the alveolar process and the root of the anterior-most caniform tooth. Twenty-eight additional semi-landmarks were placed along the outline of the bone (Fig. S1). We then performed Procrustes superimposition on all shapes; shapes were scaled to the same size and rotated to minimize distances among landmarks (Gower, 1975; Rohlf and Slice, 1990; Adams and Otárola-Castillo, 2013). Species' mean shapes were subsequently computed. We then measured the lateral area of the MXC by measuring the area of the shape defined by landmark 2 (the intersection of the ascending and alveolar processes) and the next four semi-landmarks along the ventral edge of the ascending process (Fig. S2). These measurements were taken using the program Image-J (http://imagej.nih.gov/ij/).

Associations between morphology and kinematics

We tested the hypothesis that the size of the MXC is correlated with kinematic variables of upper jaw protrusion during biting. We examined the relationship between species' mean values for the area of the MXC and three kinematic variables: time to peak premaxillary protrusion, peak premaxillary protrusion and time to jaw retraction. Exploratory analyses revealed that these kinematic variables each showed positive correlation with body size (standard length). Therefore, prior to analyses, each of these kinematic variables was phylogenetically size-corrected following Revell (2009), a method that accounts for the statistical non-independence in interspecific data (Felsenstein, 1985). For simplicity, we size-corrected variables using only the pruned maximum clade credibility (MCC) phylogeny; no other trees from Baliga and Law (2016) were sampled for size-correcting purposes. The area of the MXC was not size-corrected as premaxillary shapes had already been scaled to the same centroid size. We then performed a series of linear regressions using the area of the MXC as the independent variable in each case and size-corrected kinematic variables as the dependent variables. For each bivariate pair, we fitted an ordinary least squares (OLS) model as well as three phylogenetic generalized least squares (PGLS) models (again using the MCC tree). Each of the three PGLS models differed in their expected correlation structure: Brownian motion, Ornstein–Uhlenbeck (single optimum) and Pagel's lambda (Felsenstein, 1985; Martins and Hansen, 1997; Pagel, 1999; Freckleton et al., 2002). All models were then compared via Akaike's size-corrected information criterion (AICc) score (Burnham and Anderson, 2002).

Journal of Experimental Biology (2017) 220, 2787-2797 doi:10.1242/jeb.153783

We also tested the association between body orientation angle and the presence of a cleft in the lower lips. Lip-cleft history was inferred by first fitting macroevolutionary models of discrete evolution to our dataset. We carried out separate analyses using the MCC phylogeny as well as 100 sampled phylogenies from the posterior distribution of trees provided in Baliga and Law (2016). These analyses were accomplished via the *fitDiscrete()* function in the *geiger* package in R (Yang, 2006; Harmon et al., 2008). The best-fitting model (assessed via lowest AICc) was then used to inform stochastic character mapping on each phylogeny. We generated 100 character maps using the *make.simmap()* function in *phytools* (Revell, 2012), and then used the *densityMap()* function to summarize the posterior density for the mapped character along branches. Stochastic character mapping revealed that the lower lip cleft evolved once on all phylogenies. Thus, to avoid phylogenetic pseudo-replication, we did not make use of phylogenetic ANOVA (Garland et al., 1993). Instead, we made comparisons of species' mean body orientation angle between taxa with and without the lower lip cleft using Student's *t*-test.

Phylo-kinematic space

To ultimately quantify the extent of kinematic convergence among cleaners using multivariate data, we first generated a phylogenetically informed kinematic space. We performed phylogenetic principal components analyses (pPCA) following Revell (2009). This also allowed us to visualize the major axes of diversity of kinematic patterns across taxa. To perform the pPCAs, we sampled 100 phylogenies from the posterior distribution of trees provided in Baliga and Law (2016) as well as the MCC tree from their study. For each of the 101 pPCAs, we used data from 11 kinematic variables in total, six displacement and angular variables: body orientation angle, peak gape distance, peak premaxillary protrusion, peak hyoid excursion, peak lower jaw rotation and peak cranial rotation; and five timing variables: time to peak gape, time to peak premaxillary protrusion, time to peak hyoid excursion, time to peak cranial rotation and time to jaw retraction. Time to peak lower jaw rotation was not used as it exhibited near-collinearity with time to peak premaxillary protrusion.

We first calculated the mean data for all specified variables for each individual, and subsequently used these data to calculate species' mean values. Exploratory analyses revealed each variable to be positively correlated with standard length except for body orientation angle and peak cranial rotation. Consequently, the size-influenced data were phylogenetically size-corrected using standard length following Revell (2009). This procedure was performed separately using the MCC phylogeny and each of the 100 additional trees.

The set of phylogenetically size-corrected species' mean data and (non-size-corrected) body orientation angle and peak cranial rotation were then used in the 101 separate pPCAs to generate phylo-kinematic spaces. Each pPCA was run using the correlation matrix of traits, as variables were heterogeneous with respect to unit of measurement.

Because most traits loaded strongly along axes that appeared to separate cleaners from non-cleaners, these data were subsequently used in a series of phylogenetic ANOVA (Garland et al., 1993) to test for mean differences between cleaner and non-cleaner taxa. To account for phylogenetic uncertainty, a set of separate phylogenetic ANOVA was performed for each variable using the 101 phylogenies, with 10,000 simulations per analysis. To account for the testing of multiple hypotheses, *P*-values were corrected following methods from Benjamini and Hochberg (1995), which controls the false discovery rate.

Assessing kinematic convergence

Within each of the 101 generated phylo-kinematic spaces, we quantified convergence among all cleaner fishes; species from all three cleaner dietary groups were together identified as a group of putatively convergent taxa. We explored the extent of convergence among cleaners using one of Stayton's (2015) distance-based measures, C3, which quantifies the amount that lineages evolve to be more similar. Stayton's C3 is measured by first subtracting D_{tip} (the distance, here Euclidean, between putatively convergent taxa in phenotypic space) from D_{max} (the maximum distance between any pair of taxa in the lineages). This difference is then divided by the sum of all phenotypic distances from ancestors to descendants along the lineages leading from the most recent common ancestor (MRCA) to the specified taxa. Stayton's C3 thus ranges from 0 to 1; larger values indicate greater amounts of convergence.

We used simulation procedures (available at http://CRAN.R-project.org/package=convevol; Stayton 2014) to test for the

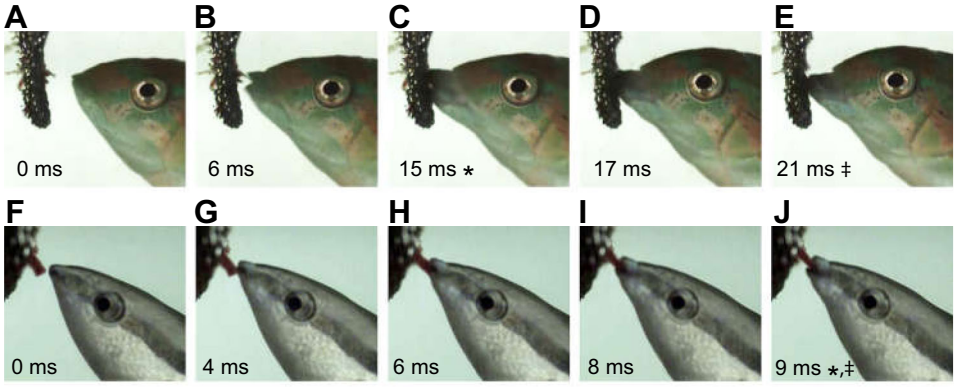

Fig. 3. Disparate styles of premaxillary protrusion among taxa in this study. Still images from videos of (A–E) *Thalassoma hardwicke* and (F–J) *Labroides dimidiatus* feeding on attached invertebrates. Anteroventral motion of the premaxilla during premaxillary biting is exhibited by *T. hardwicke* in C–E, leading to an asynchrony between the timing of peak gape (C) and peak premaxillary protrusion (E). This pattern of motion was consistently found among non-labrichthyine wrasses in this study. Labrichthyine wrasses (including *L. dimidiatus*) exhibited a simpler form of premaxillary protrusion that did not feature pronounced anteroventral motion. This style of jaw protrusion was associated with synchrony of peak gape and peak premaxillary protrusion (J) and faster jaw motions (see Results). *Peak gape, ‡peak premaxillary protrusion.

Journal of Experimental Biology

Journal of Experimental Biology (2017) 220, 2787-2797 doi:10.1242/jeb.153783

Table 1. Linear models of kinematic variables against maxillary crest area

Kinematic variable (size corrected)	Model	R^2	Slope (estimate±s.e.)	Intercept (estimate±s.e.)	*F*	*P*
Time to peak premaxillary protrusion	OLS	0.59	0.0041±0.0008	−4.6946±0.8627	24.53	0.0001
Peak premaxillary protrusion	OLS	0.73	0.0011±0.0002	−1.0441±0.1613	48.22	<0.0001
Time to jaw retraction	OLS	0.36	0.0085±0.0027	−10.4579±2.8581	9.71	0.0063

The variable listed in each row was used as the dependent variable in separate regressions against maxillary crest area. Four linear models were fitted to each set of variables: ordinary least squares (OLS) and three phylogenetic generalized least squares models (see Materials and methods for more details). The best-fit models are each described.

significance of convergence (α=0.05) among cleaners, with 1000 simulations per test. This procedure was performed separately using data from each of the 101 phylo-kinematic spaces. In each analysis, we used data from PC axes selected by an optimal coordinates stopping rule (Raîche et al., 2013) to incorporate a maximum amount of variation while excluding subsequent axes that are more likely to represent noise (Peres-Neto et al., 2005). We then fitted three macroevolutionary models to each set of PC scores using the *fitContinuous()* function in *geiger* (Harmon et al., 2008) to inform simulations. The macroevolutionary models were based on Brownian motion, Ornstein–Uhlenbeck (single optimum) and Pagel's lambda (Felsenstein, 1973; Pagel, 1999; Butler and King, 2004). Because the Brownian motion models were universally identified as the best-fitting models via AICc score, we made no alterations to Stayton's procedure (which relies on simulating phylogenetic data under Brownian motion).

RESULTS

External anatomy

Among the taxa in this study, we found *L. quadrilineatus* and both *Labroides* species to be the only taxa to feature a complete midline vertical cleft in the lower lip. Some species, such as *D. xanthurus* and *Hemigymnus melapterus*, featured partial midline vertical clefts in the lower lip. In *D. xanthurus*, two lobes could be discerned along either side of the midline. A slight indentation was apparent along the dorsal edge of the lip, but not enough to afford direct access to the teeth. In *H. melapterus*, a small separation was found along the ventral edge of the lower lip, but the dorsal margin was intact. Again, no direct access to the teeth could be afforded through this separation. No other taxa featured clefts in the lower lips. Our inference of lip-cleft history (complete clefts only) revealed the evolution of this character to likely have occurred along the branch leading to the MRCA of *Larabicus* and *Labroides* (Fig. 1A).

Patterns of premaxillary excursion

We observed two different patterns of premaxillary excursion (and ultimately biting) across the taxa in our study. In videos for all species except the four labrichthyines, we observed protrusion of the premaxilla as the upper and lower jaws adducted on the prey (i.e. biting occurred; Fig. 3; Movies 1–4). We hereafter refer to this pattern as 'premaxillary biting'. Here, peak gape typically occurred as the anterior tips of the jaws crossed the vertical plane containing the prey item. The premaxilla then descended rapidly in an anteroventral direction, contacting both the prey item and the lower jaws. The completion of this descent almost always coincided with peak premaxillary protrusion. Therefore, peak gape and peak premaxillary protrusion were temporally separated in these species (Fig. 4A–D). Labrichthyine fishes, in contrast, did not exhibit rapid anteroventral descent of the upper jaws after peak gape (Fig. 3; Movies 5,6). Instead, the upper jaws were almost fully retracted (dorsally) prior to biting. Peak gape and peak premaxillary protrusion typically occurred simultaneously and prior to the delivery of a bite (Fig. 4E,F).

Relationships between morphological and kinematic variables

We found the area of the MXC to be positively correlated with several kinematic variables (Fig. 5, Table 1). In each case, we found

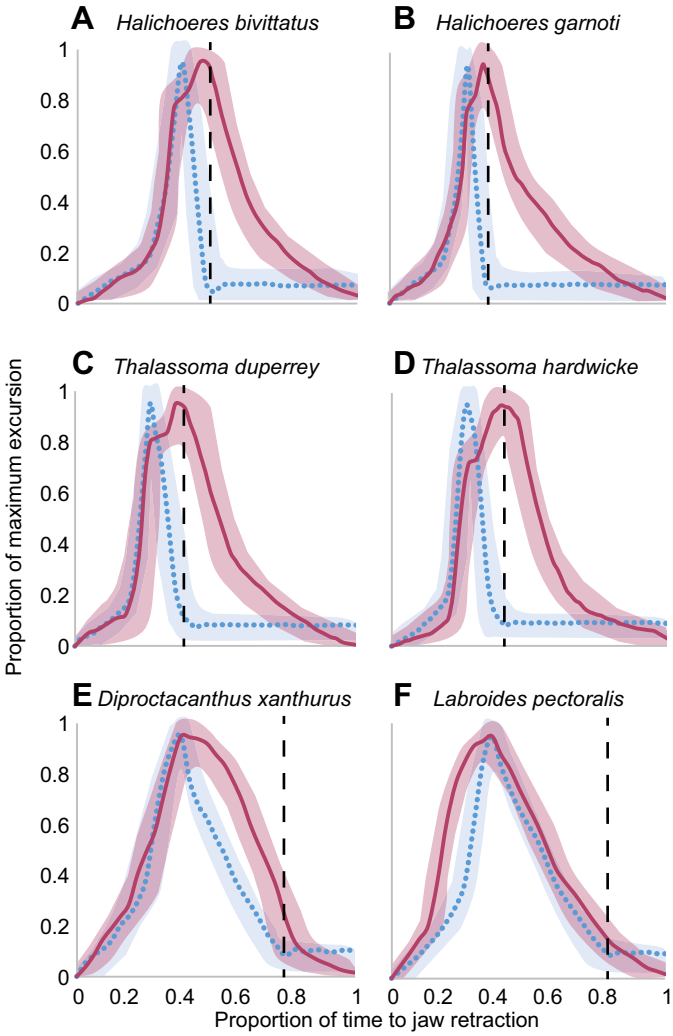

Fig. 4. Kinematic profiles of premaxillary protrusion and gape. Premaxillary protrusion (maroon, solid line) and gape (blue, dotted line) are plotted against time for 6 species of wrasses. All profiles depict species' mean trends ±s.d. Dashed vertical lines show mean time of prey capture. In non-labrichthyine species (A–D), the timing of prey capture and peak premaxillary protrusion correspond; peak gape occurs prior to this during the course of premaxillary biting. In labrichthyine taxa (E,F), peak gape and peak premaxillary protrusion occur synchronously.

Journal of Experimental Biology (2017) 220, 2787-2797 doi:10.1242/jeb.153783

OLS models to have the best fit (lowest AICc scores; Table S2). In two cases, the best-fitting PGLS model was identical to the OLS model. Regardless, all OLS and PGLS models indicated strong positive relationships between the area of the MXC and time to peak premaxillary protrusion, peak premaxillary protrusion and time to jaw retraction.

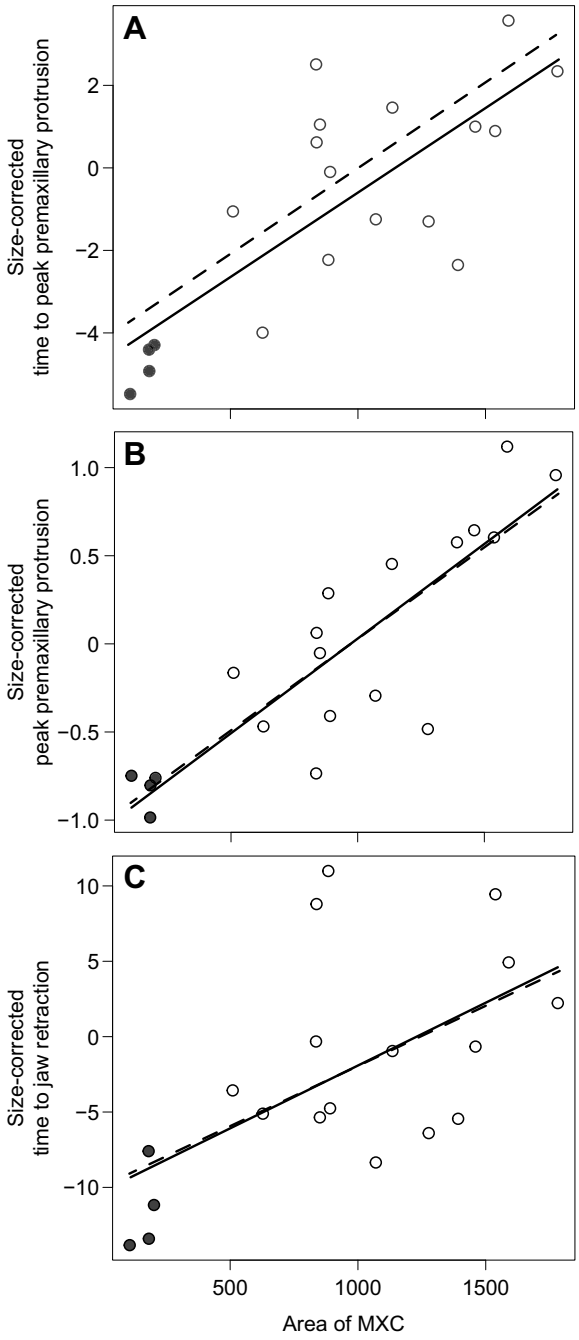

Fig. 5. Relationships between the area of the premaxillary crest and kinematic variables. Phylogenetically size-corrected (Revell, 2009) (A) time to peak premaxillary protrusion (which occurs simultaneously with prey capture in non-labrichthyine species), (B) peak premaxillary protrusion and (C) time to jaw retraction are each plotted against the relative area of the maxillary crest of the premaxilla (MXC). Regression lines depict two different linear models: ordinary least squares (solid) and the best-fitting phylogenetic generalized least squares (PGLS; dashed). Two other PGLS models were fitted to each dataset (see Materials and methods), but are not shown here. All models indicated significant, positive correlations between the variables. Filled circles show data for the four labrichthyine species.

Student's *t*-test revealed that species that exhibited a cleft in the lower lip showed significantly smaller body orientation angles (mean difference: −15.94 deg, t=−6.6190, d.f.=6.7769, P<0.0001). Although we note that group sizes were imbalanced (3 taxa with the cleft, 16 without), we found that the ranges of body orientation angles for the two groups were completely non-overlapping (Fig. 1B). Body orientation angle for individuals with the cleft ranged from 57.62 to 65.51 deg (species' mean range: 58.29–64.14 deg); angles for no-cleft individuals ranged from 65.64 to 89.40 deg (species' mean range 66.99–88.51 deg).

Phylo-kinematic space and patterns of convergence

Our generation of phylogenetic kinematic spaces allowed us to determine the major axes of kinematic variation among the 19 taxa and ultimately aided us in assessing convergence. In all 101 phylo-kinematic spaces, all traits loaded in the same direction (negatively) on PC1; loadings for the phylo-kinematic space informed by the MCC tree are shown in Table 2. On PC2, body orientation angle consistently loaded strongly and positively, while peak gape and time to jaw retraction (to a lesser extent) loaded negatively. Visualization of the primary axes of variation (Fig. 6) as a phylomorphospace (Sidlauskas, 2008) shows that cleaner fishes tend to show more positive scores on PC1 than non-cleaners.

Phylogenetic ANOVA indicated that, compared with non-cleaners, cleaner fishes showed significantly smaller magnitudes for all traits except body orientation angle and (size-corrected) peak gape distance and peak hyoid excursion (Table S3). Although cleaners, on average, also showed smaller magnitudes for these three traits, hypothesis testing indicated that the differences were not significant (body orientation angle: F=2.123, P=0.128; peak gape distance: F=2.826, P=0.084; peak hyoid excursion: F=0.376, P=0.536). For all other traits, P<0.05 even after correcting for multiple hypothesis testing.

Across all 101 phylo-kinematic spaces, the optimal coordinates stopping rule indicated that PCs 1–4 contained sufficient information for further analyses. We used scores from these PCs to assess the extent of convergence among cleaners. We found a

Table 2. Primary axes of kinematic variation in 19 species of wrasses

	PC1 (59.73%)	PC2 (10.71%)	PC3 (10.28%)	PC4 (7.59%)
Body orientation angle	−0.608	0.748	0.113	0.140
Peak cranial rotation	−0.855	0.130	0.305	0.173
Peak lower jaw angle	−0.816	0.083	−0.507	0.089
Peak gape distance	−0.648	−0.516	0.138	0.109
Peak premaxillary protrusion	−0.656	−0.261	0.536	0.162
Peak hyoid excursion	−0.446	0.207	0.381	−0.766
Time to peak gape	−0.903	0.222	−0.216	0.102
Time to peak premaxillary protrusion	−0.880	0.104	0.234	0.215
Time to peak hyoid excursion	−0.828	−0.145	−0.316	−0.198
Time to peak cranial rotation	−0.859	−0.101	−0.341	−0.227
Time to jaw retraction	−0.861	−0.356	0.019	−0.072

We performed a phylogenetically informed principal components analysis (pPCA) using the kinematic dataset and phylogenies from Baliga and Law (2016). See Materials and methods for further details. Loadings from the first four axes of the pPCA using the MCC phylogeny are shown. The percent variance for which each axis accounts is listed in parentheses in the column headings.

Journal of Experimental Biology

Journal of Experimental Biology (2017) 220, 2787-2797 doi:10.1242/jeb.153783

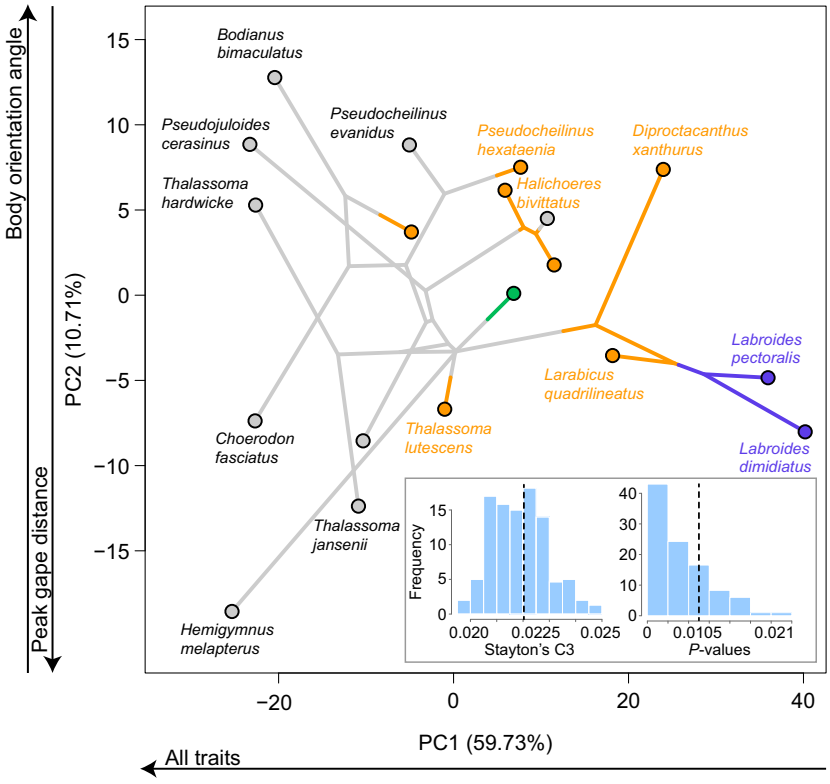

Fig. 6. Phylogenetically informed kinematic space. Phylogenetic principal components analysis (pPCA; Revell, 2009) was performed using kinematic data and each of 100 trees from the posterior distribution of Baliga and Law (2016) as well as the MCC tree. The first two axes of the pPCA performed with the MCC tree are shown here. Colors correspond to distinct characters: obligate cleaning is purple; facultative cleaning (throughout ontogeny) is green; juvenile cleaning is orange; and non-cleaning is gray. Traits that loaded strongly on each axis are represented by arrows that indicate the direction in which the magnitude of each trait increases along the axis. The inset depicts the distribution across all 101 kinematic spaces of Stayton's C3 (which quantifies the extent of convergence among cleaners) and corresponding *P*-values. Vertical dashed lines indicate the C3 metric and *P*-value for taxa in the MCC phylo-kinematic space.

Stayton's C3 value of 0.022 for the MCC phylo-kinematic space (P=0.007). The C3 values for the other 100 spaces ranged from 0.020 to 0.025 (median: 0.022). The *P*-values for these results ranged from <0.0001 to 0.021 (median: 0.003). We therefore found convergence among cleaners in all kinematic spaces.

DISCUSSION

Hypotheses of premaxillary excursion mechanisms

All species captured prey attached to a substrate via biting. Across the 19 taxa examined, videography revealed two distinct patterns of biting, predominantly driven by the motion of the premaxilla.

Cross-referencing video sequences with manipulations of freshly killed (and ultimately cleared and double-stained) specimens enabled us to document how premaxillary excursions are orchestrated during labrid biting. The two major patterns of premaxillary excursion suggest two general mechanisms by which movement of the upper jaws during biting may be accomplished.

The two mechanisms appear to initiate premaxillary movement in identical ways. Prior to jaw opening, the premaxillary condyle of the maxilla (Fig. 7A,B) is nested anterodorsally to the ascending process of the premaxilla. The dorsal face of the premaxillary condyle possesses a groove. The ventrolateral edge of the ascending process of the premaxilla lies in the same sagittal plane as the groove of the premaxillary condyle. In most taxa, the dorsolateral edge of the ascending process of the premaxilla forms a prominent crest, which we named the MXC (Fig. 7A). Rotational opening of the lower jaw spurs anterior rotation of the maxilla through ligamentous connections in a four-bar linkage mechanism (Westneat, 1990). Rotation of the maxillary arm places tension on the premaxilla–maxillary ligament, causing the premaxilla to slide anteriorly along the length of its ascending process (Fig. 7C2,D2). As this sliding occurs, the MXC slides along the groove of the premaxillary condyle on the maxilla.

In the more predominant case of premaxillary biting (shown by all taxa in the present study except the labrichthyines), this rotation of the maxilla results in the sliding of the premaxillary condyle around the MXC. Peak gape distance occurs as the MXC slides over the premaxillary condyle while the lower jaw continues to rotate open (Fig. 7C2). Peak premaxillary protrusion, however, does not occur until after the trailing edge of the MXC has slid beyond the premaxillary condyle (Fig. 7C3). For this motion to occur, however, some posterior rotation of the maxilla appears necessary. This could be the result of early activation of the A1 subdivision of the adductor mandibulae, as this is the only subdivision to insert directly onto the maxilla. Posterior rotation of the maxilla would also place tension on the premaxilla–maxillary ligament, potentially pulling the premaxilla posteroventrally. The sliding beyond the premaxillary condyle of the maxilla by the maxillary condyle of the premaxilla results in a rapid anteroventral descent of the premaxilla onto the lower jaw as peak protrusion occurs (Figs 3E and 7C3). This jaw adduction co-occurs with the delivery of a bite into the prey item.

After the premaxillary bite is delivered, the mechanism via which the jaws return to their initial position is somewhat unclear. The chief obstacle to returning the premaxilla to its original state is the positioning of the premaxillary condyle of the maxilla (Fig. 7C4); the MXC must slide over this condyle (Fig. 7C5,C6). This could be facilitated by (1) contraction of the A2 and A3 subdivisions of the adductor mandibulae (which insert onto the lower jaw), resulting in the forceful closing of the lower jaw. Rotation of the lower jaw may then push the premaxilla dorsally, guiding the MXC over the premaxillary condyle. This may occur along with or in lieu of (2) contraction of the A1 subdivision of the adductor mandibulae (which inserts on the medial face of the maxillary arm), resulting in the rotation of the maxilla back to its initial position. This rotation conceivably places tension on the premaxilla–maxillary ligament, this time pulling the premaxilla posterodorsally. Rotation of the maxilla could also free

Journal of Experimental Biology (2017) 220, 2787-2797 doi:10.1242/jeb.153783

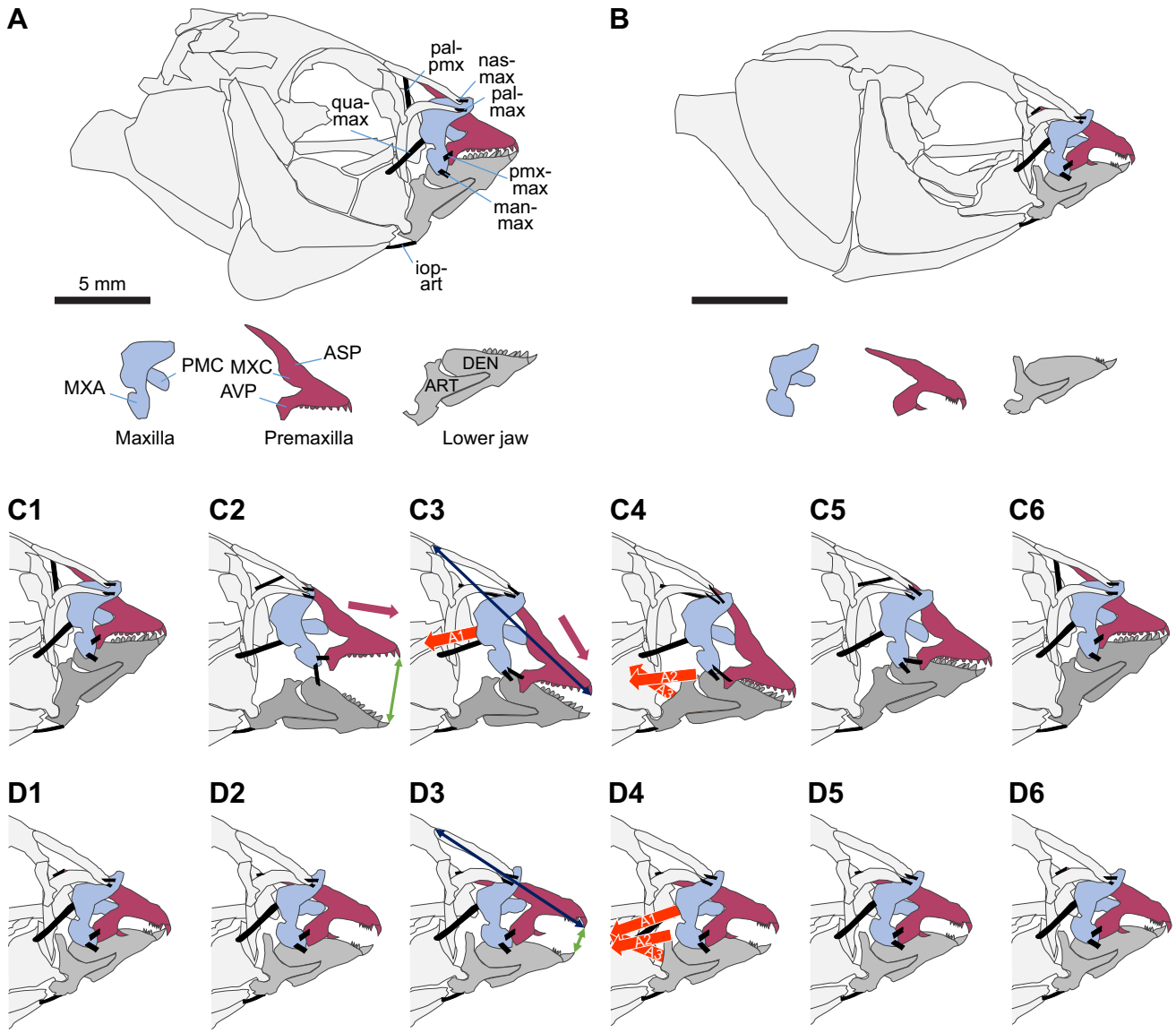

Fig. 7. Hypotheses of premaxillary excursion mechanisms during biting. (A,B) Cranial skeleton of *Thalassoma lutescens* (A) and *L. dimidiatus* (B). Bone abbreviations: ART, articular; ASP, ascending process of the premaxilla; AVP, alveolar process of the premaxilla; DEN, dentary; MXA, maxillary arm; MXC, maxillary crest of the premaxilla; PMC, premaxillary condyle of the maxilla. Ligament abbreviations: iop-art, interopercular-articular; man-max, mandibular-maxillary; pal-max, palatomaxillary; pal-pmx, palatopremaxillary; pmx-max, premaxilla-maxillary; qua-max, quadrato-maxillary. (C1–6) The hypothesis of premaxillary biting in non-labrichthyine taxa. (D1–6) The hypothesis of jaw motion in labrichthyines (see Results for more details).

the premaxillary condyle from acting as an impediment to the posterodorsal movement of the ascending process of the premaxilla.

Labrichthyine taxa appear to engage in an alternate mechanism of premaxillary motion during biting. With an absence or reduction of the MXC, the premaxilla simply slides anteriorly along the length of its ascending process, seemingly unhindered by interference from the premaxillary condyle (Fig. 7D2,D3). Here, peak gape and peak premaxillary protrusion occur simultaneously (or nearly so). Biting is accomplished by the closing of the upper and lower jaws on the prey item after peak gape and premaxillary protrusion occur (Fig. 7D4). Finally, contraction of the adductor mandibulae ushers movement of the jaws to their original positions and orientations (Fig. 7D5,D6).

Our observation of premaxillary biting in all species except for the four labrichthyines implies that its underlying mechanism is likely common to most labrids when biting for prey apprehension. That the species we examined are widely dispersed across the labrid phylogeny further supports this idea. The strong relationships between the area of the MXC and timing variables indicate that this feature is an important determinant of premaxillary movement patterning. Species with larger crests showed greater premaxillary excursions but slower movements. To further clarify the orchestration of protrusion, electromyography could be used to record the relative timing of contractions among the subdivisions of the adductor mandibulae complex. Such experiments will contribute towards our understanding of biting mechanisms in fishes.

We caution against over-interpretation of these patterns, especially in the context of labrid evolution. The observation that the labrichthyines were the only species in the present study to have reduced MXC sizes does not preclude other lineages of labrids to have undergone similar morphological trends. It is difficult to establish whether this premaxillary condition is unique to the

Journal of Experimental Biology (2017) 220, 2787-2797 doi:10.1242/jeb.153783

Labrichthyini. Moreover, it is important to note that all individuals in all species in this study were juveniles that acquired prey attached to a substrate via biting. Several taxa, including most cleaner fishes in this study, undergo ontogenetic shifts in diet (Parenti and Randall, 2000; Randall, 2005). Although changes to the feeding apparatus have been documented in some of these species (Baliga and Mehta, 2014), how kinematic patterns change over ontogeny in labrids has been little explored. How the size of the MXC and its interaction with the maxilla affect prey-capture behaviors other than biting is also unknown. Ferry-Graham et al. (2002) note the predominance of suction and ram in the behaviors of (adult-sized) labrids while feeding on attached prey items. Because of differences in the parameterization of jaw protrusion, it is difficult to know how premaxillary movements observed by Ferry-Graham et al. (2002) compare with those we document herein. Nevertheless, should fishes rely purely on suction or ram-suction and/or feed on unattached prey, the premaxilla could be employed in dissimilar ways to those we observed, even among species in the present study.

Functional mechanics of protruded biting

The premaxillary biting shown by non-labrichthyine wrasses constitutes a type of protruded biting. Biting while the jaws are protruded has been observed in a variety of fishes including mojarras (Shaffer and Rosen, 1961), sticklebacks (Anker, 1974), cichlids (Barel, 1983), butterflyfishes (Motta, 1988), angelfishes (Konow and Bellwood, 2005, 2011) and cyprinodontiform fishes (Ferry-Graham et al., 2008), but in many cases the precise mechanisms of jaw motion remain unclear. Of these taxa, only mojarras, cyprinodontiforms and some species of pygmy angelfishes (subgenus *Xiphypops* within the polyphyletic genus *Centropyge*) show anteroventrally oriented jaw protrusion during biting (Shaffer and Rosen, 1961; Ferry-Graham et al., 2008; Konow and Bellwood, 2011).

Although the direction of jaw protrusion in these taxa is anteroventral, it is likely that the mechanism of protruded biting in these groups differs from that of labrids. A feature akin to the labrids' MXC is not apparent in any of these groups. Unlike labrids, mojarras achieve anteroventral jaw protrusion via a premaxillomandibular ligament that ties the premaxilla to the lower jaw (Shaffer and Rosen, 1961). Cyprinodontiform premaxillary biting occurs through the action of a unique insertion of the A2 division of the adductor mandibulae on the premaxilla along with a unique conformation of the premaxillomandibular ligament (Hernandez et al., 2008). Both features are absent in labrids. The anteroventral premaxillary movement observed in pygmy angelfishes occurs because of a more oblique orientation of the mouth, even at rest (Konow and Bellwood, 2011). All labrids in the present study possess terminally oriented mouths. Moreover, we found patterns of premaxillary biting among (non-labrichthyine) labrids to be bi-phasic: contact with prey is made first by the upper jaws and then by the lower. Protruded biting in other groups such as pygmy angelfishes appears to be accomplished by occluding the (protruded) upper and lower jaws over prey items simultaneously (Konow and Bellwood, 2005; Konow et al., 2008).

Biting with protruded premaxillae appears to have a cost and researchers have speculated that there may be a trade-off with suction production, mainly with respect to protrusion distance and speed (Ferry-Graham et al., 2008). Barel (1983) found that a reduction in premaxillary protrusion was correlated with greater bite force across cichlids. Similarly, Motta (1988) found that butterflyfishes that tend to bite also show less jaw protrusion than relatives more prone to suction-feed. Conceivably, in cases where the direction of upper jaw protrusion is horizontal, protruding the jaws and thereafter biting could reduce bite force by (1) increasing the lever arm of the upper jaw (and thereby reducing mechanical advantage of this musculoskeletal lever) and/or (2) extending a kinetic musculoskeletal linkage network that is relatively loosely connected (and thus is less capable of withstanding forces than a fused upper jaw).

In contrast, the anteroventrally directed premaxillary biting employed by non-labrichthyines could potentially enhance the force applied to prey items during the bite. Most models of bite force (e.g. Westneat, 2003) predict force based on the actions of the A2 and A3 subdivisions of the adductor mandibulae in closing the lower jaws; the upper jaws are often not incorporated. Here, we found that during biting, the premaxilla is not simply an element that slides anteriorly along the length of its ascending process. Rather, the interaction between the premaxillary condyle of the maxilla and the MXC governs a pattern of seemingly forceful anteroventral upper jaw movement. Whether the forces produced through this premaxillary biting contribute a substantial proportion of the total force delivered through biting remains to be determined.

Furthermore, this anteroventral pattern of excursion produces a motion that allows a substantial proportion of the length of the alveolar process of the premaxilla (Fig. 7A) to potentially contact prey while biting. The anteroventral descent of the premaxilla uses a motion path that orients the alveolar process close to parallel with the mid-coronal plane as the bite is delivered. The upper jaw thus acts as a vise in clamping down on prey. Teeth that are more posteriorly situated along the alveolar process could therefore be recruited during prey capture. Although using bloodworms and mysis shrimp in our feeding trials consistently resulted in taxa using their anteriormost teeth in prey capture, capturing larger prey items may involve the use of teeth situated further along the jaws. In contrast, most labrichthyine taxa possess premaxillae that have curved alveolar processes on which the teeth are nearly all anteriorly situated (Fig. 7B) (Randall, 1958; Baliga and Mehta, 2015; P. C. Wainwright, personal communication). Through low-excursion jaw movements, only the anteriormost teeth contact prey, confining the bite to a reduced area, as noted by Baliga and Mehta (2015). This is analogous to using forceps to pick prey, where one exerts precise and localized force on an object (Ferry-Graham et al., 2008).

Evidence of specializations for cleaning in the labrichthyines

Coupled with an evolutionary reduction or complete loss of the MXC, the labrichthyine pattern of premaxillary motion featured little anteroventral motion of the upper jaws. The simpler, anteriorly directed motion of the labrichthyine premaxilla coincides with these species' exhibition of the fastest times to peak premaxillary protrusion, as well as some of the fastest overall bite cycle times. Simply put, we found that labrichthyines have economized biting by eliminating the need to overcome the MXC.

Labrichthyine taxa further distinguish themselves from other cleaner fishes. With premaxillae that show curved alveolar processes with teeth concentrated at the anterior ends, labrichthyine taxa are geared to precisely 'pick' (*sensu* Ferry-Graham et al., 2008) at prey items using forceps-like jaws. Ferry-Graham et al. (2008) posit that the increased dexterity shown by pickers requires a trade-off with speed, evidenced by cyprinodontiform pickers showing strike velocities slower than those of non-picking percomorphs. Within labrids, however, the opposite seems to be true. Picking in *Labroides* and other labrichthyines is markedly faster than biting in other

Journal of Experimental Biology (2017) 220, 2787-2797 doi:10.1242/jeb.153783

wrasses. The obligate cleaners in *Labroides* show some of the most extreme reductions in kinematic timing and excursion variables, and the closely related juvenile cleaners *L. quadrilineatus* and *D. xanthurus* show highly similar patterns. Although the extent to which non-labrichthyine cleaners should also be considered 'pickers' is less clear, we note that these taxa also showed reductions in timing and excursions compared with closely related non-cleaners.

As also noted by Baliga and Mehta (2015), the lower lip of some labrichthyines features a complete vertical cleft along the midline. This was tied to the extreme acuteness of body orientation angles shown as the predators approached prey. A substantially higher mean body orientation angle shown by *D. xanthurus* coincides with the lack of a full lip-cleft in this species. Our inference of lip-cleft history revealed the evolution of this character to likely have occurred along the branch leading to the MRCA of *Larabicus* and *Labroides*. We posit that the cleft lips of *Larabicus* and *Labroides* provide an additional 'step' towards cleaning specialization. In addition to affording easier access to medial villiform teeth, exhibiting acute body orientations also places the pectoral and pelvic fins closer to the surface of a client's body. It has been observed that *L. dimidiatus* will use its fins to placate otherwise unruly clients (Bshary and Würth, 2001; Grutter, 2004). Accordingly, approaching prey items at acute body angles could afford these cleaners a chance to bite into prey items through their midline lip-clefts while possibly using the pelvic fins to appease clientele.

We therefore find that labrichthyine taxa in general possess functional characteristics that are tied to cleaning. What remains to be seen is how any of these characters may afford advantages to corallivory. Members of the Labrichthyini are conspicuous among the Labridae for their dietary strategies. *Labroides* species are notable for being the only obligate cleaners among wrasses. Other labrichthyines, such as species in *Labrichthys* and some *Labropsis*, consume coral mucus almost exclusively (Randall, 1974; Randall and Springer, 1975; McIlwain and Jones, 1997; Parenti and Randall, 2000). Some taxa, including members of *Labropsis*, *Diproctacanthus* and *Larabicus*, even exhibit an ontogenetic dietary shift from cleaning in the juvenile phase to near-obligate corallivory in the adult (Randall, 1974, 2005; Cole et al., 2008, 2010). Thus, the evolutionary history of cleaning within the Labrichthyini is rather intertwined with that of corallivory. Adding another layer to this Gordian knot is the observation that in this clade, both cleaners and corallivores alike engage in mucivory. *Labroides* species, for example, often 'cheat' during cleaning interactions by consuming mucus off their clients (Randall, 1958; Gorlick, 1980; Bshary and Grutter, 2002). An investigation of the functional morphology of coral mucus-feeding could help disentangle how traits conducive to this strategy relate to those involved in cleaning behavior.

Cleaners show kinematic convergence

We found evidence that labrid cleaner fishes from diverse genera show patterns of kinematic convergence. Despite the unique patterns of biting exhibited by labrichthyine taxa, which resulted in some of the most extreme kinematic profiles, cleaner fishes exhibit smaller distances between each other in our multivariate kinematic spaces than their inferred historical lineages. Cleaners tended to have reduced jaw excursions coupled with faster biting behaviors compared with those of closely related non-cleaners. These patterns support speculations on cleaning made by Baliga and Mehta (2015). They proposed that taking multiple quick bites to dislodge prey may be a key feature of cleaning. Large-excursion, forceful biting by cleaner fishes could deter their clientele from acquiescing to the interaction. Additionally, patterns of convergence were apparent despite the presence of premaxillary biting in all non-labrichthyine taxa. Non-labrichthyine cleaners exhibit faster, lower-excursion movements than non-cleaners despite having the same mechanism of premaxillary biting.

In our kinematic spaces, specialist obligate cleaners (namely *L. dimidiatus* and *L. pectoralis*) exhibited some of the most extreme kinematic profiles, as indicated by their relative distances from the centroid. Along PC1, nearly all other cleaners could be found between the space occupied by the obligate taxa and the non-cleaner wrasses. Hence, it appears that all the non-specialist, facultatively cleaning taxa occupy a middle ground between non-cleaning and obligate cleaning. Though the *Labroides* appear to be pushing the boundary of kinematic space, whether taxa are ordinated along a gradient of cleaning specialization on PC1 remains unresolved. This hypothesis could be evaluated should specific data that detail the extent to which each species cleans become available.

Although at least 59 species of labrids engage in cleaning, Baliga and Law (2016) found that most evolutions of cleaning were in 5 clades of wrasses: *Bodianus*, New World *Halichoeres*, *Symphodus*, *Thalassoma* and the Labrichthyini. Our kinematic sampling contains at least one member from each of these groups except for *Symphodus*. While we caution against the over-interpretation of our results (i.e. whether findings from 10 species of cleaners can truly be generalized to the other 49), we note that our selection of taxa comprises a broad sampling of cleaning in the Labridae.

Conclusions

Through investigating feeding on attached prey in 19 species of wrasses, we found that cleaner fishes exhibit convergence in kinematics during the juvenile phase despite variation in ecological specialization. Cleaners, on average, show faster jaw movements than non-cleaners through reduced excursions. The patterns of jaw movement during biting are consistent in non-cleaners and most labrid cleaners and result in a premaxillary bite. Patterns of biting are influenced by the interaction between the premaxillary condyle of the maxilla and the MXC. The relative size of the MXC correlates with kinematic patterns. A subset of cleaners, all of which belong to the Labrichthyini tribe, exhibited reductions in MXC size, among other distinguishing characteristics. These traits coincide with a distinct style of prey capture in these labrichthyine species, leading to some of the fastest and lowest-excursion jaw movements. Therefore, we conclude that in a clade containing ecological specialists, the fundamental pattern of jaw movement during biting has been altered. Further exploring how muscle recruitment patterns orchestrate movement of the jaws may greatly enhance our understanding of the role of premaxillary protrusion during biting.

Acknowledgements

We thank M. Mac, T. Portulano and H. Hermann-Sorensen for assistance in filming animals and/or specimen preparation. C. J. Law, S. S. Kienle, B. A. Higgins, K. Dale, K. Voss and C. Jacquemetton provided valuable discussion. Special thanks to the staff of the Science Internship Program at UC Santa Cruz (R. Guhathakurtha, N. Arnberg, S. Grasso and E. Entress) for matching Z.J.B. and S.S. with V.B.B.

Competing interests

The authors declare no competing or financial interests.

Author contributions

Conceptualization: V.B.B., R.S.M.; Methodology: V.B.B.; Software: V.B.B.; Validation: V.B.B., Z.J.B., S.S., R.S.M.; Formal analysis: V.B.B.; Investigation: V.B.B., Z.J.B., S.S.; Resources: V.B.B., R.S.M.; Data curation: V.B.B.; Writing - original draft: V.B.B.; Writing - review & editing: V.B.B., Z.J.B., S.S., R.S.M.; Visualization: V.B.B.; Supervision: R.S.M.; Project administration: V.B.B., R.S.M.; Funding acquisition: V.B.B., R.S.M.

Journal of Experimental Biology

Funding
Partial funding towards animal acquisition and care and materials for clearing and staining was provided by the Rosemary Grant Award for Graduate Student Research from the Society for the Study of Evolution to V.B.B. A Committee on Research (COR; University of California Santa Cruz) Fixed Obligation Grant (FOG; 2017) to R.S.M. helped support this study.

Supplementary information
Supplementary information available online at
http://jeb.biologists.org/lookup/doi/10.1242/jeb.153783.supplemental

References

Adams, D. C. and Otárola-Castillo, E. (2013). geomorph: an R package for the collection and analysis of geometric morphometric shape data. *Methods Ecol. Evol.* **4**, 393-399.
Anker, G. C. H. (1974). Morphology and kinetics of the head of the stickleback, *Gasterosteus aculeatus*. *Trans. Zool. Soc. Lond.* **32**, 311-416.
Armbruster, W. S. (2014). Floral specialization and angiosperm diversity: phenotypic divergence, fitness trade-offs and realized pollination accuracy. *AoB Plants* **6**, plu003.
Baliga, V. B. and Law, C. J. (2016). Cleaners among wrasses: phylogenetics and evolutionary patterns of cleaning behavior within Labridae. *Mol. Phyl. Evol.* **94A**, 424-435.
Baliga, V. B. and Mehta, R. S. (2014). Scaling patterns inform ontogenetic transitions away from cleaning in *Thalassoma* wrasses. *J. Exp. Biol.* **217**, 3597-3606.
Baliga, V. B. and Mehta, R. S. (2015). Linking cranial morphology to prey capture kinematics in three cleaner wrasses: *Labroides dimidiatus*, *Larabicus quadrilineatus*, and *Thalassoma lutescens*. *J. Morphol.* **276**, 1377-1391.
Barel, C. D. N. (1983). Towards a constructional morphology of cichlid fishes (Teleostei: Perciformes). *Neth. J. Zool.* **33**, 357-424.
Benjamini, Y. and Hochberg, Y. (1995). Controlling the false discovery rate: a practical and powerful approach to multiple testing. *J. R. Stat. Soc. B* **57**, 289-300.
Bshary, R. and Grutter, A. S. (2002). Asymmetric cheating opportunities and partner control in a cleaner fish mutualism. *Anim. Behav.* **63**, 547-555.
Bshary, R. and Würth, M. (2001). Cleaner fish *Labroides dimidiatus* manipulate client reef fish by providing tactile stimulation. *Proc. R. Soc. Lond. B.* **268**, 1495-1501.
Burnham, K. P. and Anderson, D. R. (2002). *Model Selection and Multimodel Inference: A Practical Information-Theoretic Approach*, 2nd edn. Berlin: Springer-Verlag.
Butler, M. A. and King, A. A. (2004). Phylogenetic comparative analysis: a modeling approach for adaptive evolution. *Am. Nat.* **164**, 683-695.
Cole, A. J., Pratchett, M. S. and Jones, G. P. (2008). Diversity and functional importance of coral-feeding fishes on tropical coral reefs. *Fish Fish.* **9**, 286-307.
Cole, A. J., Pratchett, M. S. and Jones, G. P. (2010). Cleaning to corallivory: ontogenetic shifts in feeding ecology of tubelip wrasse. *Coral Reefs* **29**, 125-129.
Coté, I. M. (2000). Evolution and ecology of cleaning symbioses in the sea. *Oceanogr. Mar. Biol. Annu. Rev.* **38**, 311-355.
Dingerkus, G. and Uhler, L. D. (1977). Enzyme clearing of alcian blue stained whole small vertebrates for demonstration of cartilage. *Stain Technol.* **52**, 229-232.
Felsenstein, J. (1973). Maximum likelihood estimation of evolutionary trees from continuous characters. *Am. J. Hum. Genetics.* **25**, 471-492.
Felsenstein, J. (1985). Phylogenies and the comparative method. *Am. Nat.* **125**, 1-15.
Ferry-Graham, L. A., Wainwright, P. C., Westneat, M. W. and Bellwood, D. R. (2002). Mechanisms of benthic prey capture in wrasses (Labridae). *Mar. Biol.* **141**, 819-830.
Ferry-Graham, L. A., Gibb, A. C. and Hernandez, L. P. (2008). Premaxillary movements in cyprinodontiform fishes: An unusual protrusion mechanism facilitates “picking” prey capture. *Zoology* **111**, 455-466.
Freckleton, R. P., Harvey, P. H. and Pagel, M. (2002). Phylogenetic analysis and comparative data: a test and review of evidence. *Am. Nat.* **160**, 712-726.
Futuyma, D. J. and Moreno, G. (1988). The evolution of ecological specialization. *Annu. Rev. Ecol. Syst.* **19**, 207-233.
Garland, T., Jr, Dickerman, A. W., Janis, C. M. and Jones, J. A. (1993). Phylogenetic analysis of covariance by computer simulation. *Sys. Biol.* **42**, 265-292.
Gorlick, D. L. (1980). Ingestion of host fish surface mucus by the Hawaiian cleaning wrasse, *Labroides phthirophagus* (Labridae), and its effect on host species preference. *Copeia* **1980**, 758-762.
Gower, J. C. (1975). Generalized Procrustes analysis. *Psychometrika* **40**, 33-51.
Grutter, A. S. (2004). Cleaner fish use tactile dancing behavior as a preconflict management strategy. *Curr. Biol.* **14**, 1080-1083.
Haldane, J. B. S. (1951). *Everything has a History*. London: Allen & Unwin.
Harmon, L. J., Weir, J. T., Brock, C. D., Glor, R. E. and Challenger, W. (2008). GEIGER: investigating evolutionary radiations. *Bioinformatics* **24**, 129-131.
Hernandez, L. P., Ferry-Graham, L. A. and Gibb, A. C. (2008). Morphology of a picky eater: a novel mechanism underlies premaxillary protrusion and retraction within cyprinodontiforms. *Zoology* **111**, 442-454.
Konow, N. and Bellwood, D. R. (2005). Prey-capture in *Pomacanthus semicirculatus* (Teleostei, Pomacanthidae): functional implications of intramandibular joints in marine angelfishes. *J. Exp. Biol.* **208**, 1421-1433.
Konow, N. and Bellwood, D. R. (2011). Evolution of High Trophic Diversity Based on Limited Functional Disparity in the Feeding Apparatus of Marine Angelfishes (f. Pomacanthidae). *PLoS ONE* **6**, e24113.
Konow, N., Bellwood, D. R., Wainwright, P. C. and Kerr, A. M. (2008). Evolution of novel jaw joints promote trophic diversity in coral reef fishes. *Biol. J. Linn. Soc.* **93**, 545-555.
Martins, E. P. and Hansen, T. F. (1997). Phylogenies and the comparative method: a general approach to incorporating phylogenetic information into the analysis of interspecific data. *Am. Nat.* **149**, 646-667.
Martin, C. H. and Wainwright, P. C. (2011). Trophic novelty is linked to exceptional rates of morphological diversification in two adaptive radiations of Cyprinodon pupfish. *Evolution.* **65**, 2197-2212.
McIlwain, J. L. and Jones, G. P. (1997). Prey selection by an obligate coral-feeding wrasse and its response to small-scale disturbance. *Mar. Ecol. Prog. Ser.* **155**, 189-198.
Motta, P. J. (1988). Functional morphology of the feeding apparatus of ten species of Pacific butterflyfishes (Perciformes, Chaetodontidae): an ecomorphological approach. *Environ. Biol. Fishes.* **22**, 39-67.
Pagel, M. (1999). Inferring the historical patterns of biological evolution. *Nature* **401**, 877-884.
Parenti, P. and Randall, J. E. (2000). An annotated checklist of the species of the Labroid fish families Labridae and Scaridae. *Ichy. Bull.* **68**, 1-97.
Peres-Neto, P. R., Jackson, D. A. and Somers, K. M. (2005). How many principal components? Stopping rules for determining the number of non-trivial axes revisited. *Comp. Stat. Data. Anal.* **49**, 974-997.
Raîche, G., Walls, T. A., Magis, D., Riopel, M. and Blais, J. G. (2013). Non-graphical solutions for Cattell’s scree test. *Meth. Euro. J. R. Meth. Behav. Soc. Sci.* **9**, 23-29.
Randall, J. E. (1958). A review of the labrid fish genus *Labroides*, with descriptions of two new species and notes on ecology. *Pac. Sci.* **22**, 327-347.
Randall, J. E. (1974). The effect of fishes on coral reefs. *Proc. 2nd Intl. Coral. Reef. Symp.*, Brisbane, pp. 159-166.
Randall, J. E. (2005). *Reef and Shore Fishes of the South Pacific: New Caledonia to Tahiti and the Pitcairn Islands*, 707 pp. Honolulu: University of Hawai’i Press.
Randall, J. E. and Springer, V. G. (1975). The monotypic Indo-Pacific labrid fish genera *Labrichthys* and *Diproctacanthus* with description of a new related genus, *Larabicus*. *Proc. Biol. Soc. Wash.* **86**, 279-298.
Revell, L. J. (2009). Size-correction and principal components for interspecific comparative studies. *Evolution* **63**, 3258-3268.
Revell, L. J. (2012). phytools: an R package for phylogenetic comparative biology (and other things). *Methods Ecol. Evol.* **3**, 217-223.
Rohlf, F. J. and Slice, D. E. (1990). Extensions of the Procrustes method for the optimal superimposition of landmarks. *Syst. Zool.* **39**, 40-59.
Russell, B. C. (1988). Revision of the labrid fish genus *Pseudolabrus* and allied genera. *Rec. Austr. Mus. Suppl.* **9**, 1-72.
Shaffer, B. and Rosen, D. E. (1961). Major adaptive levels in the evolution of the Actinopterygian feeding mechanism. *Am. Zool.* **1**, 187-204.
Sidlauskas, B. (2008). Continuous and arrested morphological diversification in sister clades of characiform fishes: A phylomorphospace approach. *Evolution* **62**, 3135-3156.
Stayton, C. T. (2015). The definition, recognition, and interpretation of convergent evolution, and two new measures for quantifying and assessing the significance of convergence. *Evolution* **69**, 2140-2153.
Tedman, R. A. (1980a). Comparative Study of the Cranial Morphology of the Labrids *Choerodon venustus* and *Labroides dimidiatus* and the Scarid *Scarus fasciatus* (Pisces: Perciformes) I. Head Skeleton. *Aust. J. Mar. Freshwate.r Res.* **31**, 337-349.
Tedman, R. A. (1980b). Comparative Study of the Cranial Morphology of the Labrids *Choerodon venustus* and *Labroides dimidiatus* and the Scarid *Scarus fasciatus* (Pisces: Perciformes) II. Cranial Myology and Feeding Mechanisms. *Aust. J. Mar. Freshwate.r Res.* **31**, 351-372.
Westneat, M. W. (1990). Feeding mechanics of teleost fishes (Labridae; Perciformes): a test of four-bar linkage models. *J. Morph.* **205**, 269-295.
Westneat, M. W. (1994). Transmission of force and velocity in the feeding mechanisms of labrid fishes (Teleostei, Perciformes). *Zoomorphol.* **114**, 103-118.
Westneat, M. W. (2003). A biomechanical model for analysis of muscle force, power output and lower jaw motion in fishes. *J. Theor. Biol.* **223**, 269-281.
Westneat, M. W. and Alfaro, M. E. (2005). Phylogenetic relationships and evolutionary history of the reef fish family Labridae. *Mol. Phylogenet. Evol.* **36**, 370-390.
Winterbottom, R. (1974). A descriptive synonymy of the striated muscles of the Teleostei. *Proc. Natl. Acad. Sci. Phil.* **125**, 225-317.
Yang, Z. (2006). *Computational Molecular Evolution*. Oxford: Oxford University Press.

Species	BOA (°)	GAPE (mm)	PMX (mm)	LJA (°)	HX (mm)	CR (°)	TTPG (ms)	TTPMX (ms)	TTPH (ms)	TTCR (ms)	TTJR (ms)
Bodianus bimaculatus	86.61	0.97	0.60	27.13	0.21	6.67	14.05	17.15	19.31	19.51	37.18
Bodianus rufus	76.51	1.03	1.30	20.43	0.19	4.23	14.08	16.13	18.32	18.35	33.51
Choerodon fasciatus	72.51	2.93	2.11	34.3	0.28	4.73	16.21	19.89	24.82	27.48	60.51
Coris gaimard	70.63	1.97	1.73	29.64	0.23	5.64	13.43	15.16	22.75	21.15	57.05
Diproctacanthus xanthurus	75.15	1.21	0.64	12.98	0.23	3.46	11.86	12.01	13.72	16.21	31.51
Halichoeres bivittatus	77.66	1.48	1.11	18.98	0.25	4.08	12.53	15.15	17.77	19.15	34.62
Halichoeres cyanocephalus	72.82	1.52	0.92	16.48	0.22	4.42	12.15	15.08	17.37	16.51	36.51
Halichoeres garnoti	77.98	2.04	1.04	31.09	0.19	3.83	14.41	14.89	20.55	23.05	46.15
Hemigymnus melapterus	66.99	2.67	1.43	31.65	0.19	5.21	14.10	16.09	22.29	23.51	48.88
Labroides dimidiatus	58.29	1.26	0.67	13.02	0.16	2.26	10.27	11.28	15.00	15.00	30.27
Labroides pectoralis	60.15	1.30	0.62	12.98	0.17	3.01	11.15	11.95	14.70	15.68	31.05
Larabicus quadrilineatus	64.14	1.41	0.38	11.69	0.26	3.49	11.17	11.00	16.20	16.10	32.28
Pseudojuloides cerasinus	86.15	1.56	1.35	33.20	0.22	5.46	14.86	18.15	22.02	20.61	48.15
Pseudocheilinus evanidus	86.43	1.46	1.83	27.56	0.25	4.91	15.16	17.16	20.64	22.13	39.84
Pseudocheilinus hexataenia	75.15	1.33	0.93	22.10	0.18	3.70	13.64	14.65	16.63	16.15	33.08
Thalassoma duperrey	75.15	3.06	2.22	28.94	0.24	4.88	15.15	20.15	27.72	28.08	56.54
Thalassoma hardwicke	88.51	3.92	2.72	35.07	0.28	7.56	16.68	24.98	23.67	26.08	63.51
Thalassoma jansenii	70.55	4.38	2.55	33.49	0.22	5.67	16.54	23.54	23.25	25.51	60.15
Thalassoma lutescens	70.02	3.11	2.22	25.88	0.25	4.56	14.78	21.76	25.48	25.54	55.90

Table S1 – Species' mean data. Mean values for kinematic and morphological variables for each species. Abbreviations: SL, standard length; MCA, area of the maxillary crest of the premaxilla; BOA, body orientation angle; GAPE, peak gape; PMX, peak premaxillary protrusion; LJA, peak lower jaw angle; HX, hyoid excursion distance; CR, peak cranial rotation; TTPG, time to peak gape; TTPMX, time to peak premaxillary protrusion; TTPH, time to peak hyoid excursion; TTCR, time to peak cranial rotation; TTJR, time to jaw retraction

Species	SL (mm)	MCA (units^2)
Bodianus bimaculatus	38.44	836
Bodianus rufus	40.98	851
Choerodon fasciatus	63.70	1538
Coris gaimard	54.38	884
Diproctacanthus xanthurus	48.08	202
Halichoeres bivittatus	48.62	1070
Halichoeres cyanocephalus	48.51	1277
Halichoeres garnoti	64.06	628
Hemigymnus melapterus	43.25	838
Labroides dimidiatus	50.73	107
Labroides pectoralis	51.39	182
Larabicus quadrilineatus	42.86	181
Pseudojuloides cerasinus	64.91	1135
Pseudocheilinus evanidus	44.57	891
Pseudocheilinus hexataenia	39.06	510
Thalassoma duperrey	84.04	1392
Thalassoma hardwicke	77.70	1590
Thalassoma jansenii	76.47	1782
Thalassoma lutescens	73.93	1460

Table S1 (contd.)

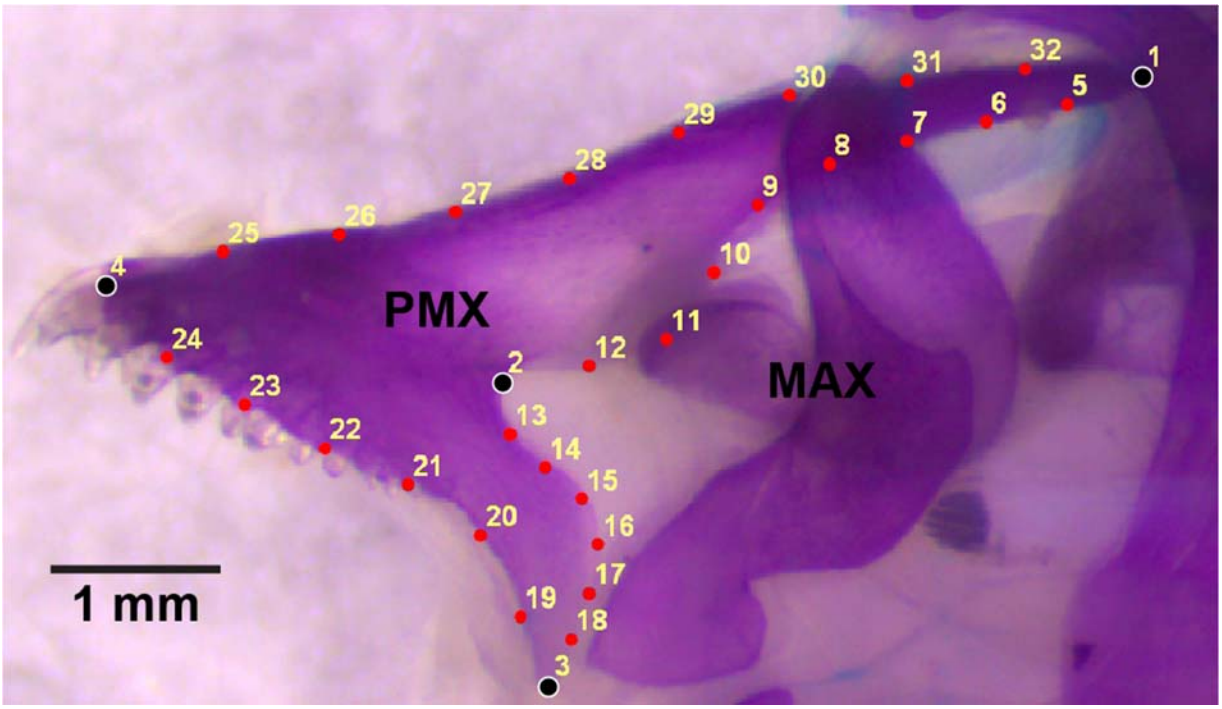

Fig. S1 – Digitization of premaxillary shape. Lateral images of the premaxilla of each specimen were imported into the program tpsDig2 (Rohlf 2006) for the placement of landmarks and semi-landmarks. Four landmarks (black) were placed on lateral photographs of each specimen, labeled as 1-4 in the figure. The landmarks were: (1) the distal end of the ascending process, (2) the intersection of the ascending and alveolar processes, (3) the distal end of the alveolar process, and (4) the root of the anteriormost caniform tooth. Twenty-eight additional semi-landmarks (red) distributed across 4 separate curves were placed along the outline of the bone (numbered 5-32 in the figure). Not shown are curves along which semi-landmarks could slide.

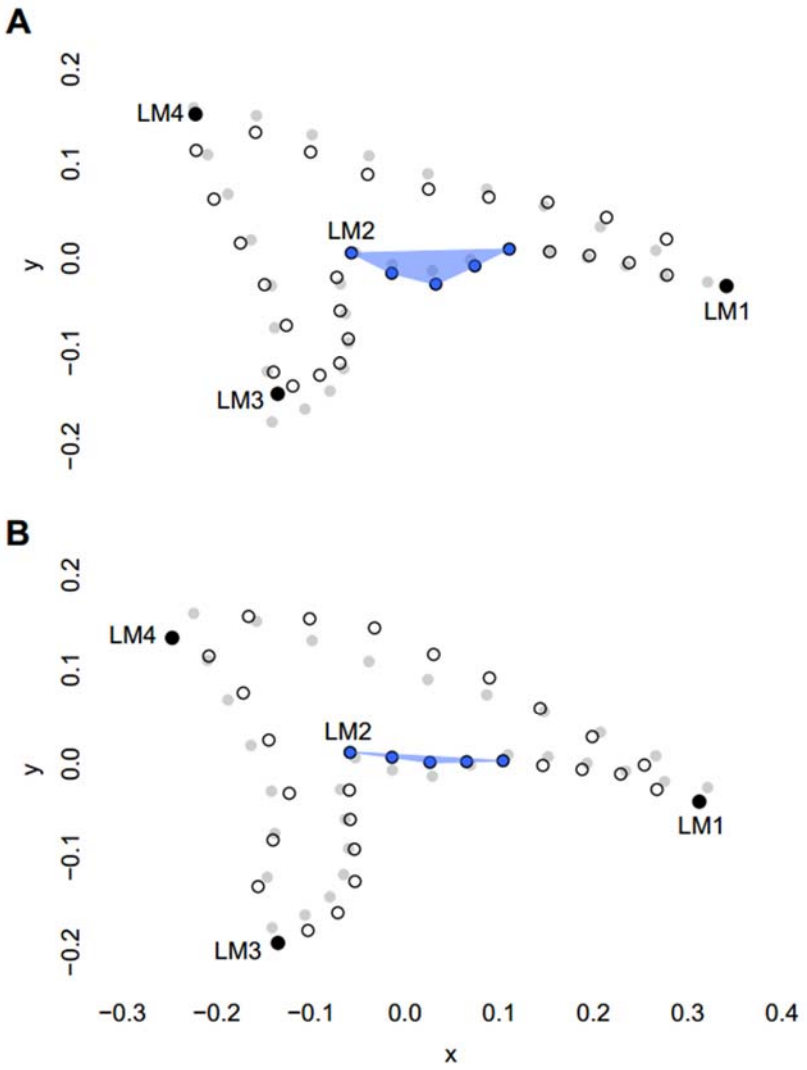

Fig. S2 – Measurement of the area of the maxillary crest. After species' mean premaxillary landmark sets were Procrustes superimposed, coordinate data were imported into the program ImageJ. The area of the maxillary crest on the premaxilla was captured by the points in blue: landmark 2 (LM2) and the next four semi-landmarks along the ventral edge of the ascending process. The area of the polygon contained within these five points was taken as a close approximation of the area of the maxillary crest. Shown above are mean landmarks for A) *Thalassoma hardwicke* and B) *Larabicus quadrilineatus*. Black, filled circles correspond to landmarks (except LM2), while open circles represent semi-landmarks (except those that capture the crest). Grey filled circles in the background of each panel show the mean shape across all species.

(Size-Corrected) Kinematic Variable	Model	ΔAICc	Slope (s.e.)	Intercept (s.e.)	Additional Parameters
Time to Peak Premaxillary Protrusion	OLS	0	0.0041 (0.0008)	-4.6946 (0.8627)	-
	PGLS – BM	8.00	0.0044 (0.0011)	-4.2969 (1.9430)	$\gamma = 1.00$
	PGLS – Pagel	1.58	0.0041 (0.0009)	-4.1632 (1.0871)	$\lambda = 0.46$
	PGLS – OU	1.67	0.0041 (0.0008)	-4.6904 (0.8613)	$\alpha = 0.46$
Peak Premaxillary Protrusion	OLS	0	0.0011 (0.0002)	-1.0441 (0.1613)	-
	PGLS – BM	5.33	0.0006 (0.0002)	-0.6037 (0.3375)	$\gamma = 1.00$
	PGLS – Pagel	0	0.0011 (0.0002)	-1.0441 (0.1613)	$\lambda = 0.00$
	PGLS – OU	1.81	0.0010 (0.0001)	-0.9352 (0.1730)	$\alpha = 0.09$
Time to Jaw Retraction	OLS	0	0.0085 (0.0027)	-10.4579 (2.8581)	-
	PGLS – BM	3.47	0.0044 (0.0034)	-4.3672 (5.7082)	$\gamma = 1.00$
	PGLS – Pagel	0	0.0085 (0.0027)	-10.4579 (2.8581)	$\lambda = 0.00$
	PGLS – OU	1.70	0.0080 (0.0032)	-8.7515 (3.3363)	$\alpha = 0.09$

Table S2 – Comparisons of linear models fit to kinematic variables against maxillary crest area. The kinematic variable listed in the first column was used as the dependent variable in separate regressions against maxillary crest area (see Figure 7 for scatter plots). Four linear models were fit to each bivariate set: ordinary least squares and three phylogenetic generalized least squares (PGLS) models. All PGLS models were informed by the MCC phylogeny. Models were compared using AICc scores. Abbreviations: OLS – ordinary least-squares; PGLS – phylogenetic generalized least squares; BM – Brownian motion; OU – Ornstein-Uhlenbeck

(Size-Corrected) Kinematic Variable	Mean Difference	F-Ratio	p-value	Corrected p-value
Body Orientation Angle	-7.980	2.123	0.128 (0.115-0.176)	0.128 (0.115-0.176)
Peak Cranial Rotation	**-1.711**	**9.021**	**0.004 (0.003-0.009)**	**0.009 (0.008-0.014)**
Peak Lower Jaw Angle	**-13.112**	**21.969**	**0.001 (0.001-0.001)**	**0.005 (0.005-0.005)**
Peak Gape Distance	-0.695	2.826	0.084 (0.078-0.108)	0.095 (0.089-0.119)
Peak Premaxillary Protrusion	**-0.515**	**4.301**	**0.043 (0.028-0.050)**	**0.044 (0.029-0.051)**
Peak Hyoid Excursion	-0.006	0.376	0.536 (0.351-0.616)	0.525 (0.351-0.616)
Time to Peak Gape	**-2.082**	**10.462**	**0.003 (0.001-0.007)**	**0.009 (0.007-0.015)**
Time to Peak Premaxillary Protrusion	**-2.845**	**5.409**	**0.023 (0.017-0.034)**	**0.035 (0.029-0.046)**
Time to Peak Hyoid Excursion	**-2.646**	**5.660**	**0.017 (0.012-0.021)**	**0.031 (0.020-0.042)**
Time to Peak Cranial Rotation	**-3.520**	**7.300**	**0.009 (0.009-0.015)**	**0.016 (0.016-0.022)**
Time to Jaw Retraction	**-10.382**	**21.084**	**0.001 (0.001-0.003)**	**0.004 (0.004-0.007)**

Table S3 – Phylogenetic ANOVAs of kinematic data. Phylogenetic ANOVA was performed for each variable listed in the first column to compare mean data between cleaners and non-cleaners. To account for phylogenetic uncertainty, the MCC phylogeny and 100 additional phylogenies from the posterior distribution of Baliga and Law (2016) were used (separately) to perform analyses. Exploratory analyses revealed each variable to be positively correlated with standard length except for: body orientation angle and maximum cranial rotation. The size-influenced data were thus size-corrected using standard length following Revell (2009). Shown in each cell are results from the ANOVA using the MCC tree with ranges for additional analyses in parentheses (values for Mean Difference and F-Ratios were nearly invariant and are thus not shown). Mean Difference was calculated by subtracting non-cleaner data from cleaner data; negative values thus indicate cleaner fishes possess smaller trait magnitudes on average. In the final column, p-values are corrected using methods from Benjamini and Hochberg (1995) to control the false discovery rate. Bold rows indicate significant differences between cleaners and non-cleaners.

Supplementary Movies

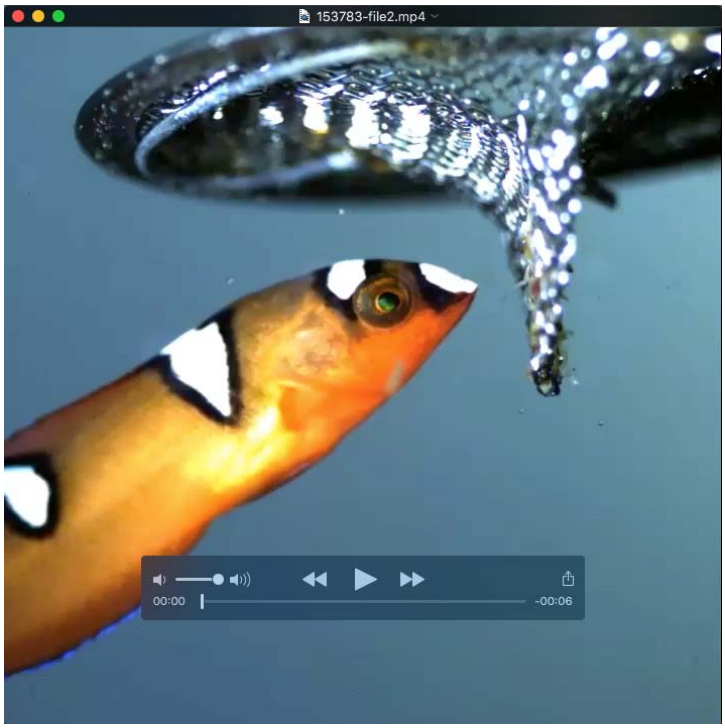

Movie 1 – *Coris gaimard* feeding on attached invertebrates and exhibiting a 'premaxillary bite'.

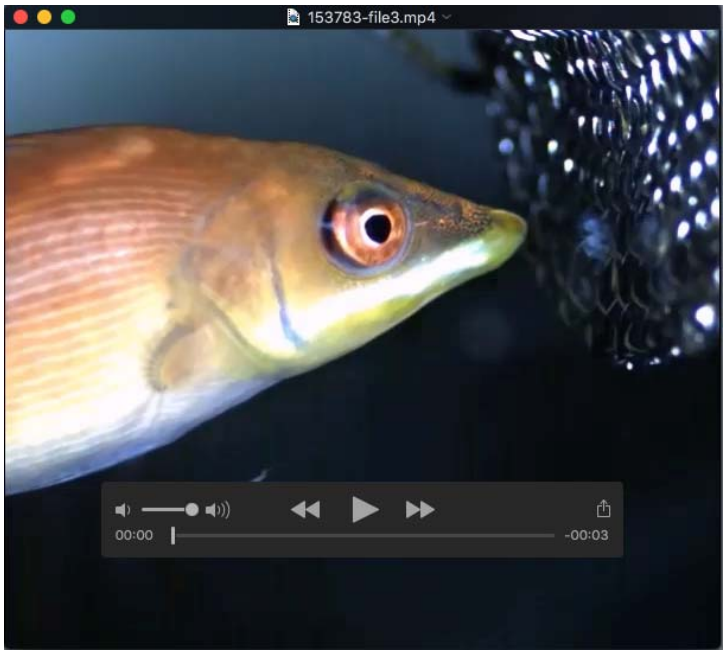

Movie 2 – *Pseudocheilinus evanidus* feeding on attached invertebrates and exhibiting a 'premaxillary bite'.

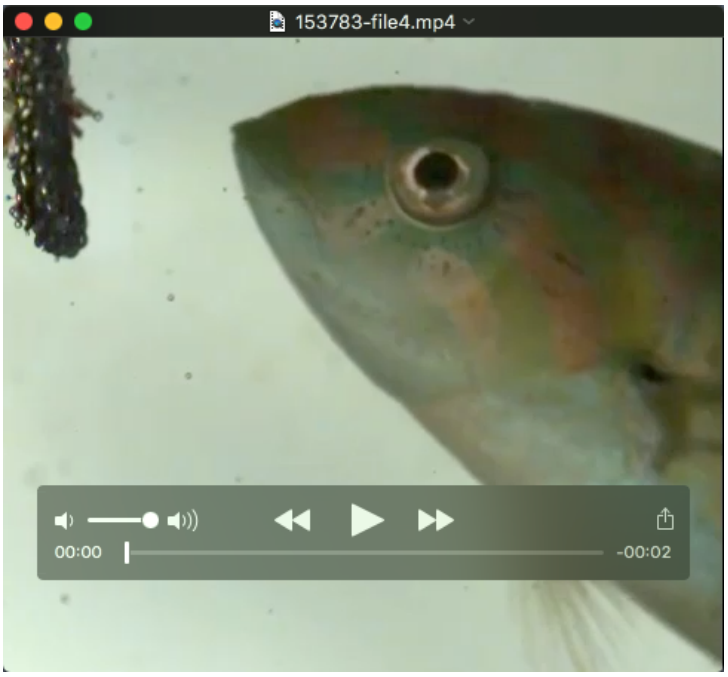

Movie 3 – *Thalassoma hardwicke* feeding on attached invertebrates and exhibiting a 'premaxillary bite'.

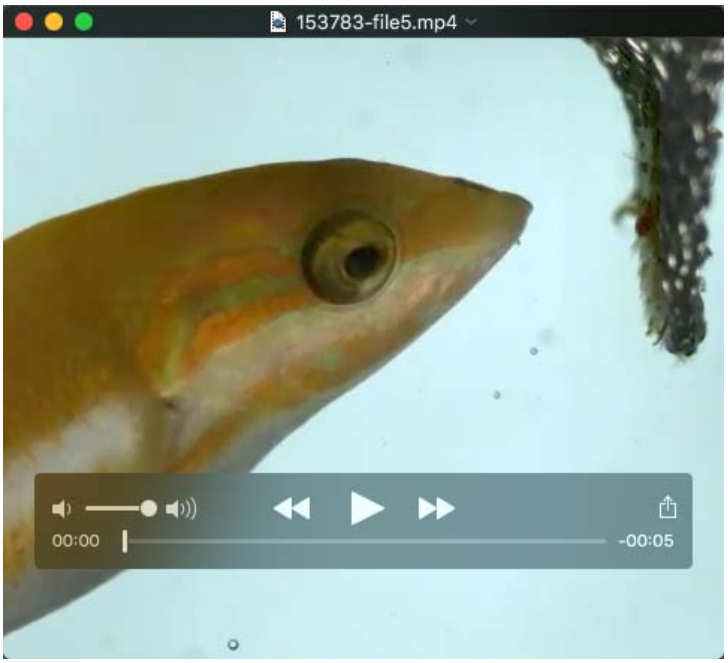

Movie 4 – *Thalassoma lutescens* feeding on attached invertebrates and exhibiting a 'premaxillary bite'.

Movie 5 – *Labroides dimidiatus* feeding on attached invertebrates. No rapid anteroventral decent of the premaxilla is apparent as the bite is delivered.

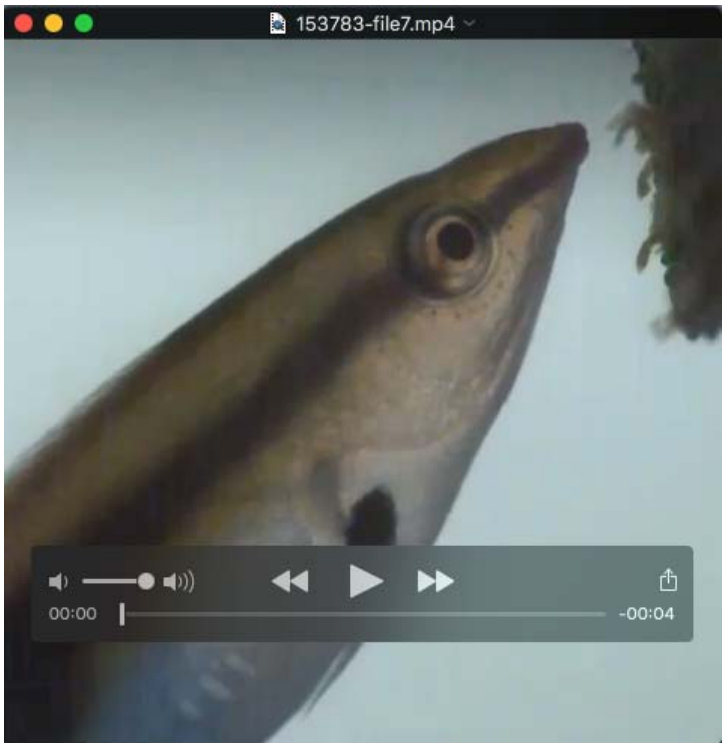

Movie 6 – *Labroides pectoralis* feeding on attached invertebrates. No rapid anteroventral decent of the premaxilla is apparent as the bite is delivered.